Sensitivity Enhancement for Surface Plasmon Resonance Imaging Biosensor by Utilizing Gold–Silver Bimetallic Film Configuration

Liangping Xia · Shaoyun Yin · Hongtao Gao ·
Qiling Deng · Chunlei Du

Abstract Gold–silver bimetallic film configuration is brought forward to realize surface plasmon resonance imaging (SPRI) biosensor with the virtues of both high sensitivity and chemical stability. The theoretical calculation is adopted to optimize the thicknesses of the metal films, and bimetallic film configuration with high refractive index sensitivity and a good linearity between reflectivity and refractive index is presented. Then, the property of the detection system is discussed. The results show that in comparison to most commercial SPRI biosensors which use single gold films, the sensitivity and molecule detection ability of the gold–silver bimetallic film configuration can be improved to a great extent. For the substrate of BAK3 glass used in this paper, the sensitivity enhancement reaches as high as 80%, which makes it a much better choice for SPRI biosensing applications.

Keywords Biosensor · SPRI · Bimetal film · Sensitivity

Introduction

Surface plasmon resonance (SPR) is tightly relative to the local refractive index on the metal layer surface, and it is highly sensitive to the refractive index change [1]. The optical sensor based on this mechanism has been a simple and direct method for the refractive index measurement, and it has been a widely used technology in biological sensing [2–5]. SPR sensing technique can be used to realize the real-time monitoring of the biologic–chemical interaction happening on the metal surface, and it needs no labeling and fluorescence of the biomolecules. Generally, there are three kinds of work modes for SPR sensing. For the first mode, the metallic film is illuminated by polychromatic light with incident angle fixed, and the refractive index information of the medium on the metal layer surface is obtained by measuring the surface plasmon resonance wavelength [6, 7]. For the second mode, the wavelength of incident light is fixed, and the refractive index change is obtained by measuring the change of the resonance incident angle [8–10]. For the third mode, both the wavelength and the incident angle are fixed, and the refractive index information is obtained by measuring the intensity change of the reflected light [11]. Compared to the former two working modes, the third one does not need spectrum measurement or mechanical circumgyration, hence, it is simple and low cost. The most important is that the sensing area can be divided into hundreds of subareas to construct multi-channels, and the real-time information of refractive index change in every subarea can be monitored by imaging devices (such as CCD, CMOS, etc.) [12, 13], hence, the SPR biosensor based on the third mode possesses the highest throughput, which is suitable for the analysis of a mass of biological samples at the same time. Due to these advantages, the third test mode possesses the highest test efficiency, which is usually called the surface plasmon resonance image (SPRI) sensing technique.

In order to acquire more exact results, the SPRI configuration should possess high sensitivity, good linearity, and high chemical stability at one time. In another words, the SPRI configuration should generate a remarkable intensity change of the reflective light when the refractive index on the metal layer is changed, this change should be linear so that the data processing will be

L. Xia · S. Yin · H. Gao · Q. Deng · C. Du (✉)
Institute of Optics and Electronics,
Chinese Academy of Sciences,
Chengdu 610209, China
e-mail: cldu@ioe.ac.cn

convenient. And, it also should be stable under various kinds of chemical conditions. Among varieties of commonly used metals, gold film is the most general choice in SPRI sensor for its chemical stability and capability of biologic molecule adhesion [14], but SPRI sensing device based on gold film does not own high sensitivity. Silver film is a good candidate for SPRI sensing because of its high SPR excitation efficiency leading to high sensitivity, but it is easy to be oxygenized in natural condition. A reasonable idea can be generated by employing gold–silver bimetallic nanofilm configuration owning the virtues of both gold film and silver film. B. H.Ong et al. analyzed bimetallic silver–gold film configuration for high sensitivity surface plasmon resonance sensing and achieved a narrow resonance full-width-half-maximum and evanescent field enhancement [15]. However, the sensing mechanism is based on the relationship between the reflectivity and the incident angle, which works in the second work mode and is not suitable for the multi-channel and imaging sensing. For SPRI sensing system which works in the third work mode, the conclusions of SPR biosensor cannot be applied directly, since the sensitivity and linearity of refractive index–reflectivity should be considered synchronously.

In this paper, gold–silver bimetallic nanofilm structure is proposed to build a SPRI sensor with high sensitivity and good linearity. The design method for optimizing the metal film thickness is theoretically studied. By establishing the relationship of the slope of the reflectivity–refractive index curve and the linearity property to the metal film thickness, the optimized thickness of the gold and silver films and the optimal incident angle are obtained. Additionally, the influence of the sensitivity enhancement to the molecule detection ability and the measurement range of the refractive index are further discussed.

Design of the Gold–Silver Bimetallic Nanofilm Configuration Based on SPRI Biosensor

In refractive index test of SPRI biosensor configuration, the Kretschmann prism is a commonly used assistant for the surface plasmon polarizations (SPPs) excitation on the metal film surface [16, 17], as shown in Fig. 1, where SPPs cannot be excited when the metal surface is illuminated directly by incident electromagnetic wave. If the transverse magnetic (TM)-polarized electromagnetic wave with wavelength λ incidents onto the surface of the prism, SPR occurs when the x-component of incident wave vector k_x equals to the SPR vector k_{sp} [18]. In this condition, the incident electromagnetic energy transforms into SPPs almost totally, and the reflection field is close to zero. When the refractive index of the medium on the metal surface changes, the resonance condition will change, finally leading to the change of the intensity of the reflective light. For instance, special biological molecules (antibody) are prepared on the metal surface beforehand, as shown in Fig. 1, when the antibody binds with the target antigen in the analyte, the effective refractive index on the metal surface will change, and the concentration information that the target antigen molecule contained in the analyte can be detected by measuring the change of the reflected light intensity.

Figure 1 shows the sketch map of the proposed SPRI biological sensor based on gold–silver bimetallic nanofilm structure. A layer of silver film is prepared before the gold film is evaporated. Gold film keeps the biosensor to be chemically stable and capable for biological molecule accretion, and silver film at the inner layer provides the high sensitivity. For the four-layer structure like prism (layer 1)/silver film (layer 2)/gold film (layer 3)/biologic molecule layer (layer 4), based on the Fresnel reflection formula [15], the reflectivity is shown below,

$$R_{1234} = \left| \frac{r_{12}^P + r_{23}^P \exp(i2k_{z2}d_2) + r_{34}^P \exp(i2k_{z2}d_2)\exp(i2k_{z3}d_3) + r_{12}^P r_{23}^P r_{34}^P \exp(i2k_{z3}d_3)}{1 + r_{12}^P r_{23}^P \exp(i2k_{z2}d_2) + r_{23}^P r_{34}^P \exp(i2k_{z3}d_3) + r_{12}^P r_{34}^P \exp(i2k_{z2}d_2)\exp(i2k_{z3}d_3)} \right|^2 \tag{1}$$

Where, for TM polarization wave,

$$r_{ij} = \frac{Z_i - Z_j}{Z_i + Z_j} \tag{2}$$

$Z_i = \varepsilon_i/k_{zi}$, $k_{zi} = k_0\sqrt{\varepsilon_i - \varepsilon_1 \sin^2(\theta)}$, ε_i is the dielectric constant of the ith layer.

In the SPRI sensing system, by assuming the test range of the refractive index is (n_L, n_H), the sensitivity can be defined as the following formula,

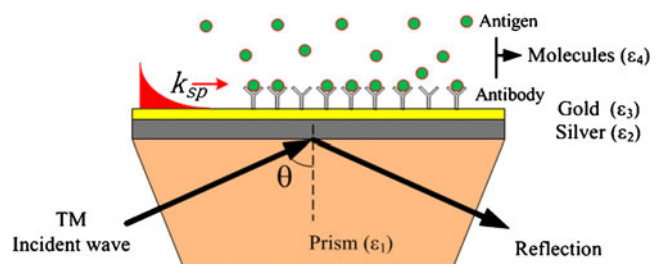$$S = |R(n_H) - R(n_L)|_{max}/\Delta n \tag{3}$$

Fig. 1 Sketch map of the SPRI biosensor based on gold–silver bimetallic nanofilm configuration

Equation 3 means the maximal intensity change of the reflective light was caused by per unit change of the refractive index when the refractive index changes from n_L to n_H, namely, S is the slope of the reflectivity–refractive index curve. The greater the intensity variation of reflective light per refractive index unit, the larger the slope is, and the more sensitive the biosensor is. The value of θ corresponding to the S is the fixed incident angle. In order to make the measurement and data processing convenient, the reflectivity–refractive index curve should be linear in the test range of refractive index. Equation 4 gives the definition of the linearity,

$$L_D = \{[R(n_H) - R(n_{mid})] - [R(n_{mid}) - R(n_L)]\}/(S \cdot 0.5 \Delta n) \quad (4)$$

where $n_{mid} = (n_L + n_H)/2$. This formula means that the linearity of the SPRI biosensor will be better when the value of L_D is closer to zero.

When the metal material and configuration of the SPRI biosensor are chosen, the sensitivity S and linearity L_D can be calculated for different thicknesses of the gold film and silver film by using Eqs. 1, 3, and 4. The theory calculation results are shown in Fig. 2. In the calculation, the incident light is the He–Ne laser with wavelength λ=632.8 nm. The coupling prism is made from BAK3 glass whose refractive index is 1.545. The dielectric constant of silver and gold is $-15.9183 + i*1.0757$ and $-9.3418 + i*1.1159$, respectively [19], the test range of the refractive index is chosen to be (n_L, n_H)=(1.33, 1.34) by the references [20, 21]. Both thicknesses of the gold and silver films range from 5 nm to 70 nm. In the sensitivity calculation result (Fig. 2a), there are two high sensitivity regions. The first one (zone A) is on the left-down corner where the thicknesses of gold and silver films are thinner than 15 nm. In this region, the value of sensitivity S is generally larger than 40/RIU, and the highest value is 53.37/RIU corresponding to the thicknesses of gold film and silver film which are 5 nm. The other high sensitivity region (zone B) is in the region where the thickness of gold film ranges from 5 nm to 20 nm and the thickness of silver film ranges from 35 nm to 60 nm. The highest value of sensitivity S is 54.84/RIU, corresponding to the thickness of gold film, which is 5 nm, and the thickness of silver film, which is 47 nm. To achieve a high sensitivity, the fixed incident angle of 67.07° is determined by solving the Eq. 3 according to the selected measuring range of refractive index.

Figure 2b shows the calculated linearity result. It can be seen that the values of L_D are usually greater than 70% in zone A. Further calculation reveals that since the thicknesses of the metal films are both very thin, most of the incident light can transmit from the metal films directly, as the incident angle increases, total reflection suddenly
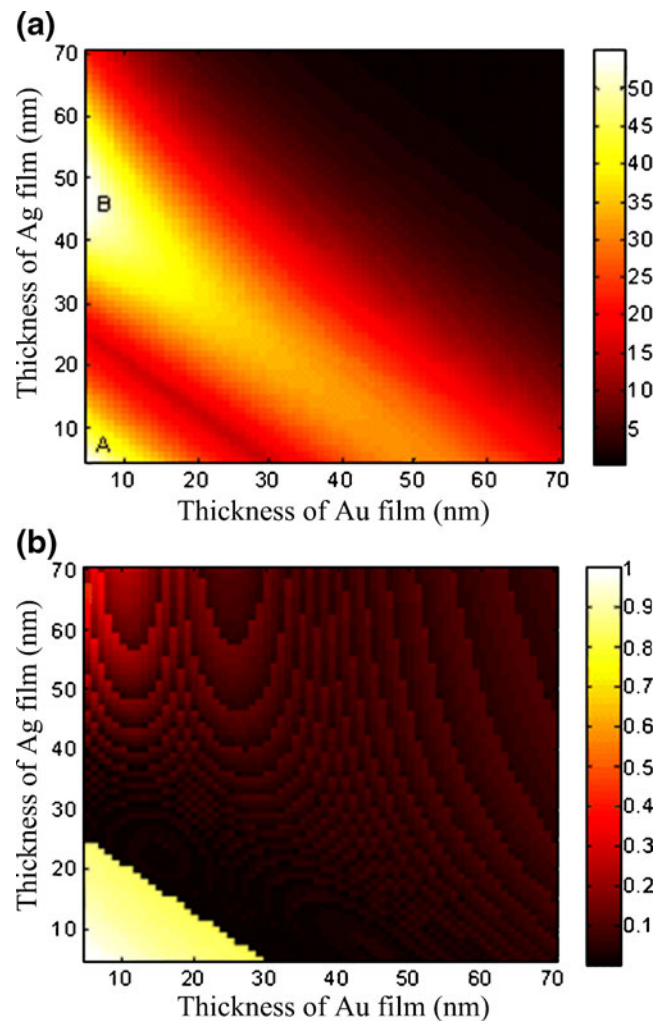

Fig. 2 The relationship between the thickness of gold–silver film and the sensitivity S (**a**) and the linearity L_D (**b**). In **a** and **b**, the *horizontal coordinate* represents the thickness of gold film, the *vertical coordinate* represents the thickness of silver film. The *color* shows the values of the sensitivity S or the linearity L_D; the closer the color is to dark part, the smaller the value is, the closer the color is to the bright part, the larger the value is

occurs, resulting in quick reflectivity change within a small angle range. The incident angle for the maximum sensitivity corresponds to the total reflection angle, and at this time, there is no SPR on the metal surface. Besides, because of the bad linearity of the reflectivity variation versus the refractive index, it is not a good choice for qualitatively refractive index measurement, thus, zone A is not fit for the SPRI biosensor in this metal film thickness region. In the zone B, the calculated linearity L_D shown in Fig. 2b is generally smaller than 1%, and the most optimized thickness of the gold and silver film is 5 nm and 47 nm, respectively.

For the single gold film-structured SPRI biosensor, the same analysis is carried out. The obtained highest sensitivity is only 30% when the optimized thickness of the gold

film is 55 nm. It means that the sensitivity of the proposed gold–silver bimetallic SPRI biosensor is 80% higher than the single gold film biosensor.

Discussion and Analysis

From the above discussions, on the condition of considering the sensitivity and linearity of refractive index–reflectivity synchronously, the optimized metal film thicknesses are obtained. In order to research the influence of the sensitivity enhancement to the whole detection system, the properties of both the sensing structures on each optimized geometrical parameters are analyzed.

The Measurement Range

To characterize the influence of the refractive index test range when the sensitivity is enhanced, the reflectivity–refractive index curves are calculated. Figure 3 shows the results. It demonstrated that the linearities of the gold–silver bimetallic sensor and the single gold film sensor are both excellent when the refractive index test range is from 1.33 to 1.34 as expected. As the test range of the refractive index increases, the slope of the reflectivity–refractive index curve of the gold–silver bimetallic configuration gets close to zero rapidly. When the refractive index of analyte is larger than 1.36, the variation of the reflective index nearly causes no intensity variation of the reflected light, thus, the bimetallic film configuration biosensor cannot be used at this condition. For the single gold film sensor, the slope of the reflectivity–refractive index curve gets smaller as the refractive index of analyte increases, but the trend is much slower than that of the gold–silver bimetallic biosensor, hence, the refractive index test range can be larger.
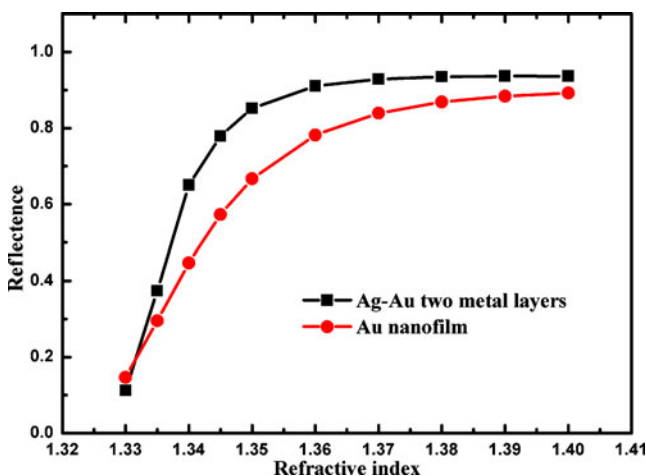

Fig. 3 The reflectivity–refractive index curves of the gold–silver bimetallic SPRI biosensor and the single gold film biosensor in their optimized geometrical parameters, respectively

Sensitivity

To further discuss the sensitivity enhancement, the field distributions in the films are calculated by Maxwell equations. For the TM mode incident wave, only the field components E_x, E_z, H_y are nonzero. And the following relationship is satisfied:

$$E_x = -i \frac{1}{\omega \varepsilon_0 \varepsilon_i} \frac{\partial H_y}{\partial z} \tag{5}$$

$$E_z = -i \frac{\beta}{\omega \varepsilon_0 \varepsilon_i} H_y \tag{6}$$

$$H_y = A_i e^{i\beta x} e^{k_i z} + B_i e^{i\beta x} e^{-k_i z} \tag{7}$$

where $k_i^2 = \beta^2 - k_0^2 \varepsilon_i$, $k_0 = \omega/c$ is the wave vector in free space, ε_i is the dielectric constant of the ith layer, and $\beta = k_x$ is the propagation constant.

When the prism is used as a coupler, the SP wave vector is $k_{sp} = \beta = \sqrt{\varepsilon_1} k_0 \sin \theta_s$, where θ_s is called the SPR angle, namely the incident angle at the interface of the prism/metal when the reflectivity calculated by Eq. 1 is the lowest. Based on the continuity of H_y and E_x, the function group about A_i, B_i is set. Here, there is only transmission field in the molecule layer. On condition of the optimized sensitivity and linearity, the metal film thicknesses and the incident angle are fixed, thus, the normalized electric field distributions of the gold–silver bimetallic structure and the single gold film structure are calculated and the results are shown in Fig. 4a and b, respectively. The red lines reveal the comparative values of the electric field intensity in each layer. The electric field intensity decreases exponentially away from the interface of the metal/molecule in the metal layer and the molecule layer, and reaches the maximum value at the interface, which reveals that the SPPs are excited at the interface of metal/molecule.

When the single gold film structure was changed to silver–gold bimetallic structure, the SPPs excitation was changed. Comparing Fig. 4(a) with Fig. 4(b), the maximum electric field of the localized mode shown at the metal/molecule interface reveals that the SPPs excitation intensity of the gold–silver bimetallic structure is larger than the single gold structure, hence, the interaction between the electromagnetic field and the molecules is stronger, which leads to the sensitivity enhancement.

Simultaneously, the attenuation length of the bimetallic structure is $L_{Ag+Au} = 199$ nm, which is longer than that of single gold film structure ($L_{Au} = 161$ nm). It means that the localized electric field can penetrate into the molecule layer deeper for the bimetallic structure, which is very advantageous to the detection of some analytic molecules with
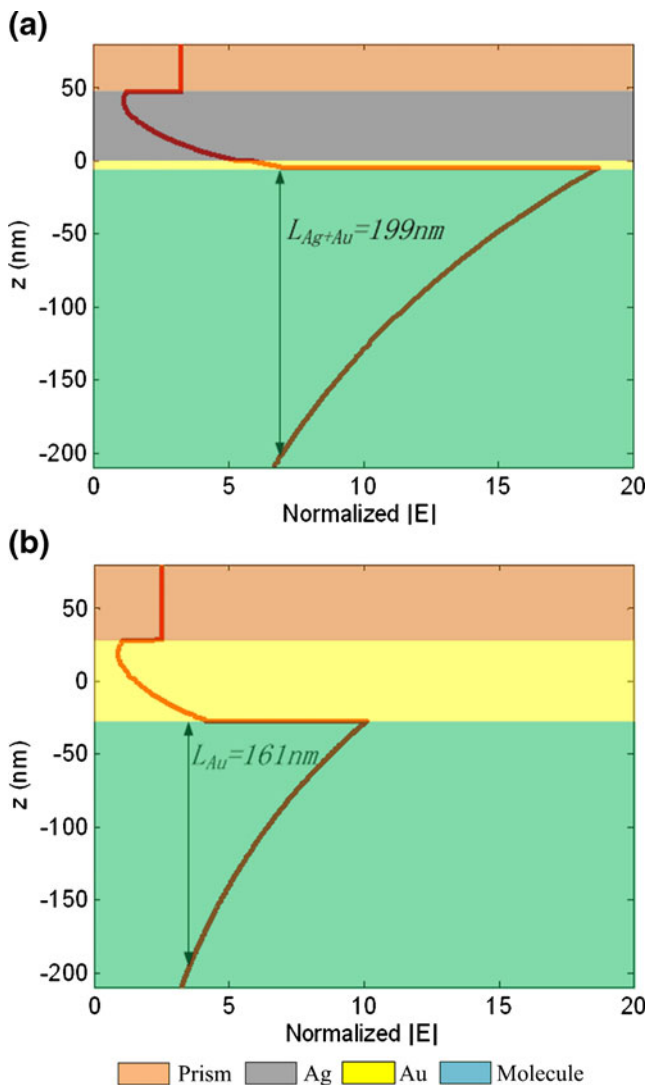
Fig. 4 The normalized electric field distribution of (**a**) the gold–silver bimetallic film structure and (**b**) the single gold film structure. The *red line* stands for the comparative values of the electric field intensity. The attenuation length L is the distance to the interface of metal/molecule when the electric intensity is decreased to 1/e in molecule layer

large dimension due to the fact that more parts of the molecules can act with the electromagnetic wave. Accordingly, the detection ability of the sensing chip with bimetallic structure is extended as expected.

Conclusion

The theory result demonstrates that the sensitivity of the SPRI biosensor can be greatly enhanced by utilizing the gold–silver bimetallic nanofilm structure, which possesses good linearity synchronously at the optimized parameters.

The further analysis results reveal that the sensitivity enhancement will extend the detection ability when analyzing molecules with large dimension but will decrease the refractive index test range. Considering the chemical stability and molecule adhesion, the single gold film configuration is generally used to excite SPPs in practical SPRI biosensor. By changing the single film to gold–silver bimetallic nanofilm, the sensitivity of the SPRI biosensor can be greatly enhanced while keeping the chemical stability and molecule adhesion, which is very important and meaningful in the precision improvement for SPRI sensing device.

References

1. Homola J, Yee S, Gauglitz G (1999) Surface plasmon resonance sensors: review. Sens Actuators, B 54(1–2):3–15
2. Karlsson R, Falt A (1997) Experimental design for kinetic analysis of protein–protein interactions with surface plasmon resonance biosensors. J Immunol Meth 200(1–2):121–133
3. Myszka D (1997) Kinetic analysis of macromolecular interactions using surface plasmon resonance biosensors. Curr Opin Biotechnol 8(1):50–57
4. Rich R, Myszka D (2000) Advances in surface plasmon resonance biosensor analysis. Curr Opin Biotechnol 11:54–61
5. Ligler FS, Taitt CR (2008) Optical biosensors: today and tomorrow, ch. 4. Elsevier, Oxford
6. Homola J, Dostalek J, Chen S, Rasooly A, Jiang S, Yee S (2002) Spectral surface plasmon resonance biosensor for detection of staphylococcal enterotoxin B in milk. Int J Food Microbiol 75:61–69
7. Haes A, Van Duyne R (2004) A unified view of propagating and localized surface plasmon resonance biosensors. Anal Bioanal Chem 379:920–930
8. Byun K, Kim S, Kim D (2005) Design study of highly sensitive nanowire-enhanced surface plasmon resonance biosensors using rigorous coupled wave analysis. Opt Express 13:3737–3742
9. Kim D (2006) Effect of resonant localized plasmon coupling on the sensitivity enhancement of nanowire-based surface plasmon resonance biosensors. J Opt Soc Am A 23:2307–2314
10. Byun K, Yoon S, Kim D, Kim S (2007) Experimental study of sensitivity enhancement in surface plasmon resonance biosensors by use of periodic metallic nanowires. Opt Lett 32:1902–1904
11. Gan Q, Bartoli F (2009) Surface-plasmon-coupled semiconductor diode-laser package for refractive index sensing. Opt Lett 34:2180–2182
12. Berger C, Beumer T, Kooyman R, Greve J (1998) Surface plasmon resonance multisensing. Anal Chem 70:703–706
13. O'BrienII MJ, Pérez-Luna VH, Brueck SRJ, López GP (2001) A surface plasmon resonance array biosensor based on spectroscopic imaging. Biosens Bioelectron 6:97–108
14. Kordesch ME, Hoffman RW (1983) Strongly adhesive gold electrodes on Melinex. Thin Solid Film 107:365–371
15. Ong B, Yuan X, Tjin S, Zhang J, Ng H (2006) Optimised film thickness for maximum evanescent field enhancement of a bimetallic film surface plasmon resonance biosensor. Sens Actuators, B 114:1028–1034

16. Quail J, Rako J, Simon H (1983) Long-range surface-plasmon modes in silver and aluminum films. Opt Lett 8:377–379

17. Kabashin A, Nikitin P (1998) Surface plasmon resonance interferometer for bio-and chemical-sensors. Opt Commun 150:5–8

18. Gryczynski I, Malicka J, Gryczynski Z, Lakowicz J (2004) Surface plasmon-coupled emission with gold films. J Phys Chem B Condensed Phase 108:12568–12574

19. Palik E, Ghosh G (1985) Handbook of optical constants of solids. Academic, New York

20. Yan S, Fang Y, Yu X (2009) Narrow beam SPR biosensor and experimental study. BMEI, pp. 1–5

21. Byun KM, Yoon SJ, Kim D, Kim SJ (2007) Experimental study of sensitivity enhancement in surface plasmon resonance biosensors by use of periodic metallic nanowires. Opt Lett 32(13):1902–1904